Fluid flow-based description of the geometrical features in fluidic channels using the Shannon’s information theory: an exploratory study

JOURNAL: Microfluidics and Nanofluidics

Brief Communication

Fluid flow-based description of the geometrical features in fluidic channels using the Shannon's information theory: an exploratory study

S. Ripandelli[1*], D. Pugliese[2*], M. Sotgiu[1], U. Morbiducci[1]

[1]Politecnico di Torino, Department of Mechanical and Aerospace Engineering, 10129 Torino, Italy

[2]Politecnico di Torino, Department of Applied Science and Technology and RU INSTM, 10129 Torino, Italy

*corresponding authors: simone.ripandelli@gmail.com; ORCID: 0000-0001-7867-9461

diego.pugliese@polito.it; ORCID: 0000-0002-6431-1655

Keywords

Shannon Entropy, microfluidics, information theory, thermodynamics, fluids

Abstract

Inspired by Nature, where storing information is an intrinsic ability of natural systems, here we investigate the capability of interacting systems to transport/store the information generated/exchanged in the interaction process in the form of energy or matter, preserving it over time. In detail, here we test the possibility to consider a fluid as a carrier of information, speculating about how to use such information. The final goal is to demonstrate that information theory can be used to illuminate physical observations, even in those cases where the equations describing the phenomenon under investigation are intractable, are affected by a budget of uncertainty that makes their solution not affordable or may not even be known. In this exploratory work an information theory-based approach is applied to microfluidic data. In detail, the classical study of the fluid flow in a microchannel with obstacles of different geometry is faced by integrating fluid mechanics theory with Shannon's theory of information, interpreted in terms of thermodynamics. Technically, computational fluid dynamics simulations at Reynolds' numbers (Re) equal to 1 and 50 were carried out in fluidic channels presenting obstacles with rectangular and semicircular shape, and on the simulated flow fields

the Shannon's information theory was applied evaluating the fluid dynamics information entropy content. It emerged that the Shannon Entropy (SE) evaluated at the outflow section of the flow channel depends upon the geometric features (i.e. position, shape, aspect ratio) of the obstacles. This suggests an interpretation of the fluid dynamics establishing in a flow channel presenting obstacles in terms of information theory, that can be used to identify *a posteriori* the geometric features of the obstacles the fluid interacts with. The proposed approach can be applied to flow data at the boundaries of fluid domains of interest to extract information on the process occurring inside a system, do not making any appeal to the governing equations of the phenomenon under observation or intrusive measurements.

1 Introduction

In principle, the behavior of fluids in motion can be fully described by three equations: an equation describing the conservation of mass, a second equation based on the second Newton's law of motion, and a third equation based on the conservation of energy (Cox 2015; Khasanov 2011; Merdasi et al. 2018).

A condition for a real fluid to be in motion is that sufficient energy is to be spent. It follows that the fluid in motion is a system that modifies its internal energy, thus generating a variation of entropy (S) of the system in a purely thermodynamic meaning. The concept of entropy (not univocally accepted indeed), which can be explained as the level of disorder of a system describing its evolution under the effect of the external environment, was taken up by Claude Shannon in 1948 (Shannon 1948) and applied to the field of information theory in order to describe the level of complexity of a signal in data communication systems. In general, it is still uncommon to apply information theory for the purpose of the analysis of flow fields characterized by different levels of complexity (Ikeda and Matsumoto 1986). Indeed, the idea of considering a fluid in motion as an information carrier is not new, inspired by the fact that Nature uses fluids to transport a plethora of biochemicals. Looking at a fluid in motion as an information carrier (e.g. nutrients to cells, proteins through blood, etc.), a parallelism between fluid flow and information theory based on the definition of the SE can be easily established.

Motivated by the possibility of interpreting a fluid as information carrier, in this study information theory is applied to microfluidics, where its capability to discriminate the shape of obstacles in a channel based on the knowledge of the motion of fluid particles upstream and downstream of the obstacle is tested. In detail, the capability of the SE to discriminate the shape of the obstacle based on the distortion of fluid streamlines is tested, with the final aim to use the SE of the system as a *fingerprint* of the obstacle shape-specific flow perturbation. The potency of the herein proposed approach has not been largely explored. To cite a valuable example, Pozo et al. (Pozo et al. 2017) analyzed the flow complexity in open systems, approaching the distortion of fluid streamlines in a channel at the level of information transmission.

Technically, here computational fluid dynamics (CFD) solutions of laminar flow in channels presenting obstacles were compared to an “ideal communication” channel where the transmitted and received messages are identical and SE was applied to CFD data. The characterization of microflows as information carriers finds several applications, e.g. to assess mixing efficiency in micromixers (Camesasca et al. 2006; Pennella et al. 2010; Pennella et al. 2012) or in microreactors and in scaffolds and bioreactors for tissue engineering applications (Eijkel and Van den Berg 2005; Bilen and Yapici 2002; Yojina and Ngamsaad 2010; Tariq et al. 2020) and in many other technological fields like solar energy (Ali 2020), nanofluids for manufacturing processes (Wang et al. 2020), heat and mass transfer (Chen et al. 2020; Sajjad et al. 2020; Sözen et al. 2021).

The principal aim of this study, and the reason of its novelty, was to investigate the behavior of a fluid that flows in a channel in presence of obstacle/s characterized by different shape, multiplicity and disposition and employing the information theory. This exploratory study highlights that at defined conditions a simplified approach based on the information theory can be applied to extract information on the processes occurring within closed systems, and that this can be done by measuring only the “information” at systems’ boundaries.

2 Methods

In this study a microchannel geometry without and with obstacles of different shape and position was investigated. Overall, as depicted in Fig. 1, nine configurations were considered, i.e. one without obstacles and 8 with obstacles. The ratio between the height of the channel h_{ch} and the characteristic obstacle dimension h_1 was set to $h_1 = h_{ch}/6$. In microchannel configurations where more than one obstacle was considered, inter-distance was set equal to $h_{ch}/2$ (Fig. 1).

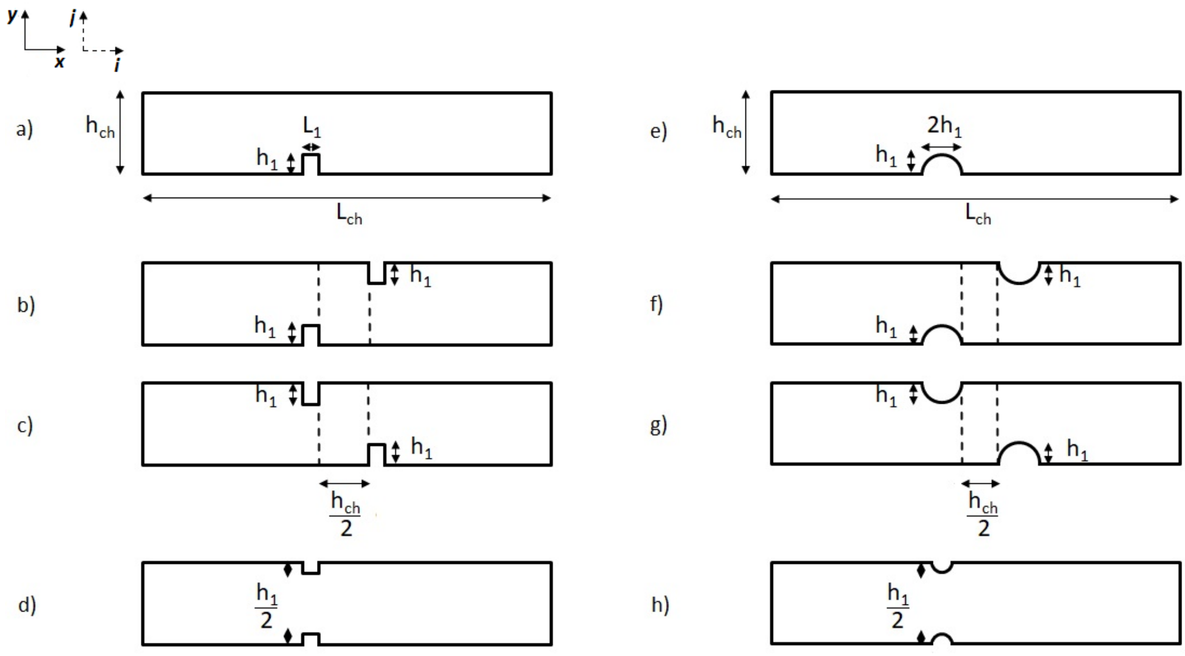

Fig. 1 Schematic illustration of the investigated channel geometries with obstacles ($h_1 = h_{ch}/6$). The analysis on models a, d, e and h is presented in the Results Section. Coordinates (*i, j*) correspond to the logical coordinates useful for the computational analysis

The analytical solution of the fluid motion in the microchannel without obstacles can be easily obtained from Navier-Stokes equations. In detail, for an incompressible, homogeneous, Newtonian fluid in steady-state laminar condition, the law of motion in the microchannel can be expressed as:

$$u_x = -\frac{1}{2\mu} \cdot \frac{dp}{dx} \cdot (y_0^2 - y^2) \; (1)$$

where u_x is the velocity in axial (x, see Fig. 1) direction, μ the dynamic viscosity, p the pressure, y the general position in vertical direction (Fig. 1) and y_0 the coordinate of the microchannel wall, where velocity is equal to 0 (i.e. no-slip conditions).

The finite volume-based CFD commercial code Fluent (ANSYS Inc., USA) was adopted to solve the discretized governing equations of fluid motion in microchannels with obstacles. In detail, the Navier-Stokes equations in their discretized form and under steady-state laminar conditions were solved using a second order pressure discretization and a second order upwind momentum discretization scheme. The fluid was assumed to be isotropic, incompressible and Newtonian with a density value ρ equal to 998.2 [kg·m^{-3}] and a dynamic viscosity μ equal to 10^{-2} [kg·s·m^{-2}]. To ensure grid-independence of the solution, based on a mesh sensitivity analysis, quad-mesh with elements size of $1 \cdot 10^{-4}$ m was adopted. On average, the resulting computational grids consisted of 24000 elements and 24381 nodes. Two different flow regimes, characterized by *Re* equal to 1 and 50, were simulated by applying Dirichlet conditions at the inflow section of the microchannel geometry (in terms of flat velocity profile), while the reference pressure Neumann boundary condition was imposed at the outflow section. Walls were assumed to be rigid, and the no-slip condition was imposed.

The concept that a confined fluid in motion is an information carrier, and the parallel with a communication system, was translated into a scheme where: (1) the fluid in the microchannel is the carrier; (2) the inflow section (or more in general a section upstream of the channel segment presenting obstacles) is the transmitter; (3) the outflow section (or more in general a section downstream of the channel segment presenting obstacles) is the receiver; (4) the difference in flow features between the two sections is the information transmitted. In this regard, flow perturbations induced by the presence of obstacles can be regarded as the "noise" affecting the system (Fig. 2). The channel without obstacles was considered as the reference case, i.e. the case where the carrier (fluid) is not disturbed and the transmitted information is not modified.

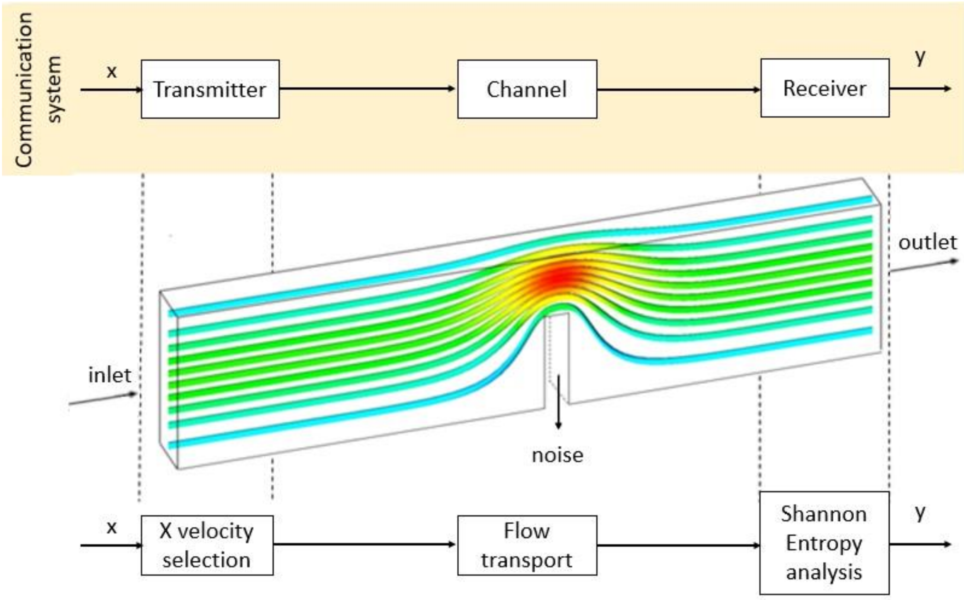

Fig. 2 Schematic illustration of the parallelism between a communication system and a fluidic system

Distilling in fluid mechanics terms, at the very low *Re* laminar flow regimes adopted in microfluid applications the streamlines deflection induced in the channel by the presence of an obstacle does represent a modification of the information content carried by the fluid at any channel location upstream of the obstacle. In the absence of obstacles, fluid streamlines will not be deflected, following a linear path; any obstacle capable to perturb the flow will deflect fluid streamlines and ultimately the carried information, in accordance with the conceptual model of Fig. 1. It is well known from the analytical solution of the laminar fluid motion in the channel without obstacles, that the flow field is characterized by streamlines parallel to the axis of the conduit (as well as to the channel's walls). The presence of an obstacle, even maintaining laminar conditions, will perturb the flow with the consequence that streamlines will be deflected losing their parallelism. This behavior was translated building up a binary matrix, representative of the phenomena. To build up the representative binary matrix, here fluid velocity data from CFD simulations were considered (i.e. for each cell of the quad-mesh a value of velocity was extrapolated). Technically, a $N\,x\,M$ matrix $B_{i,j}^{x}$ was built:

$$B_{i,j}^{x} = \begin{bmatrix} b_{1,1} & \cdots & b_{1,M-1} \\ \vdots & \ddots & \vdots \\ b_{N,1} & \cdots & b_{N,M-1} \end{bmatrix} \quad (2)$$

with $i = \{1, \dots N\}$, where N is the number of grid cells in y direction, and $j = \{1, \dots M-1\}$, where M is the number of grid cells in x direction (Fig. 1). The binary elements $b_{i,j}$ of the matrix were calculated as follows:

$$b_{i,j} = \begin{cases} 1, & \frac{\bar{u}_{i,j}^{x}}{\bar{u}_{i,j-1}^{x}} \le \zeta_{i,j} \\ 0, & otherwise \end{cases} \quad (3)$$

where $\bar{u}_{i,j}^{x}$ and $\bar{u}_{i,j-1}^{x}$ are the values of the x-component of the velocity at grid cell location (*i, j*) and (*i, j-1*), respectively. The threshold values $\zeta_{i,j}$ for matrix $B_{i,j}^{x}$ binarization were set according to:

$$\zeta_{i,j} = \frac{\bar{u}_{i,j}^{num.}}{\bar{u}_{i,j-1}^{num.}} - \frac{\bar{u}_{i,j}^{ana.}}{\bar{u}_{i,j-1}^{ana.}} = 0 \quad (4),$$

and depend on the results of CFD analysis and Eq. (1). From this equation, $\bar{u}_{i,j}^{num.}$ and $\bar{u}_{i,j}^{ana.}$ are the CFD and the analytical velocity values in x direction at grid cell location (*i, j*), and $\bar{u}_{i,j-1}^{num.}$ and $\bar{u}_{i,j-1}^{ana.}$ are the CFD and the analytical velocity values in x direction at grid cell location (*i, j-1*), respectively.

Here the SE was employed to quantify the level of interaction between fluid flow and the obstacles in the microchannel, intended as the level of streamlines deflection with respect to the microchannel without obstacles, binarized according to matrix $B_{i,j}^{x}$. By definition, the formulation of the SE is given by:

$$SE(X_i) = -P(X_i)\, log_2\, P(X_i) \quad (5),$$

where X_i is a discrete random variable with possible values $\{X_1, \ldots, X_n\}$ and $P(X_i)$ is the probability distribution of X_i. Theoretically, an increase of entropy corresponds to a loss in information content. In this study, the SE was evaluated according to:

$$SE = -P_i\, log_2\, P_i \quad (6)$$

where P_i is given by:

$$P_i = \frac{\sum_1^j b_{i,j}}{N} \quad (7)$$

Based on Eqs. (6) and (7), the SE ranges between zero (i.e. no information lost or, for the specific application, no distortion of fluid streamlines) and one (i.e. all the information carried by the fluid lost due to the disruption of the flow field as a consequence of its interaction with obstacles in the microchannel).

3 Results

The analysis was extended to all the microchannels with different obstacles geometry and number summarized in Fig. 1. As first explanatory example, the SE values computed along two cross-sections (proximal and distal to the obstacle, respectively) of the two microchannels with single obstacles of rectangular and semicircular shape, at two different Re numbers (1 and 50), are presented in Fig. 3. At $Re = 1$, as expected, moderate differences are highlighted by the SE both between the upstream and downstream sections (flow field distortion consequence of the presence of the obstacle) and between the two microchannels (consequence of the different shape of the obstacles). Marked differences in SE distribution (and in absolute values as well) along the cross-sections emerge at $Re = 50$ (Fig. 3): as expected, the presence of the rounded (semicircular) obstacle, which is expected to distort fluid streamlines less than the obstacle with rectangular shape, modifies trans-obstacle SE values markedly less than the rectangular single obstacle (the semicircular shape maintains almost unaltered the SE of the system even increasing the inertial effects by one order of magnitude, as stated by the Re). The results of Fig.

3 confirm the capability of the SE of discriminating between obstacle shapes, properly capturing thermodynamically-induced variations in the microchannel system.

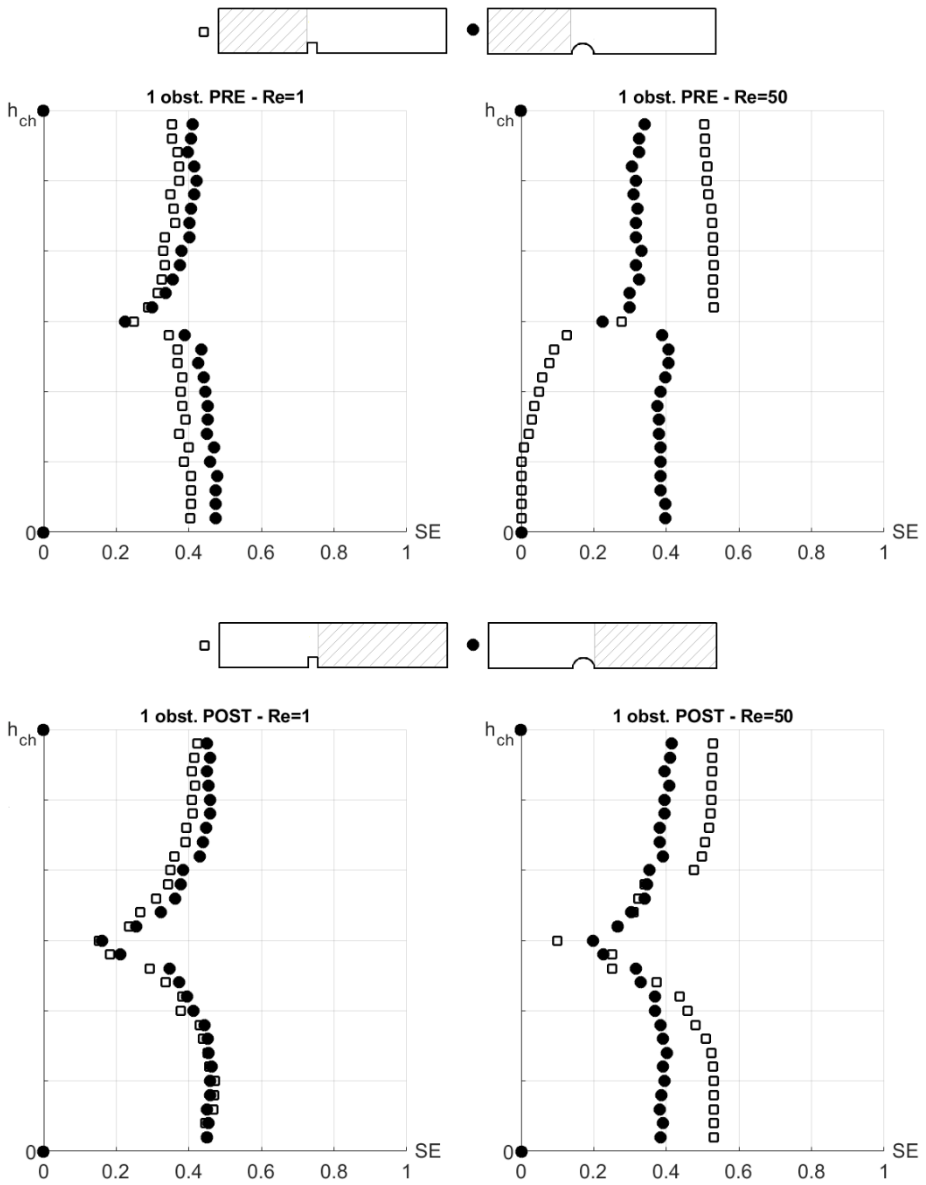

Fig. 3 SE computed on two cross-sections (proximal to the obstacle, upper panel; distal to the obstacle, lower panel) of two microchannels presenting single obstacles with different shape (rectangular and semicircular), at two different *Re* (1 and 50). h_{ch} is the general height of the channel

Figure 3 also highlights an expected lack of symmetry (more pronounced at $Re = 50$) in the SE cross-sectional distribution, reflecting the absence of geometrical and fluid dynamical symmetry in the two microchannels with single obstacles. In this regard, the second explanatory example of Fig. 4 reports the SE values computed along two cross-sections (proximal and distal to the obstacle, respectively) of the two microchannels presenting obstacles with rectangular and semicircular shape, symmetrically located with respect to the microchannel axis. In this case, the cross-sectional SE distributions: (1) confirm the capability of capturing the different influence of the shape of the obstacle in the flow field, with marked differences related to the obstacle shape clearly evident also at $Re = 1$; (2) adequately reflect the presence of a geometrical (and fluid dynamical) symmetry of the microchannel system.

Summarizing, the cross-sectional distributions of Figs. 3 and 4 clearly demonstrate that SE is an indirect measure of the impact that obstacles with different shape and configuration have on the microchannel fluid dynamics, suggesting that SE can be adopted to *a posteriori* discriminate the shape of obstacles (e.g. cultured cells in biomicrofluidic applications) in systems without optical access. This is like to say that SE can be used as a sort of *fingerprint* that specific obstacles leave on fluid streamlines, depending upon their shape, configuration and fluid dynamics conditions (as defined by the Reynolds' number).

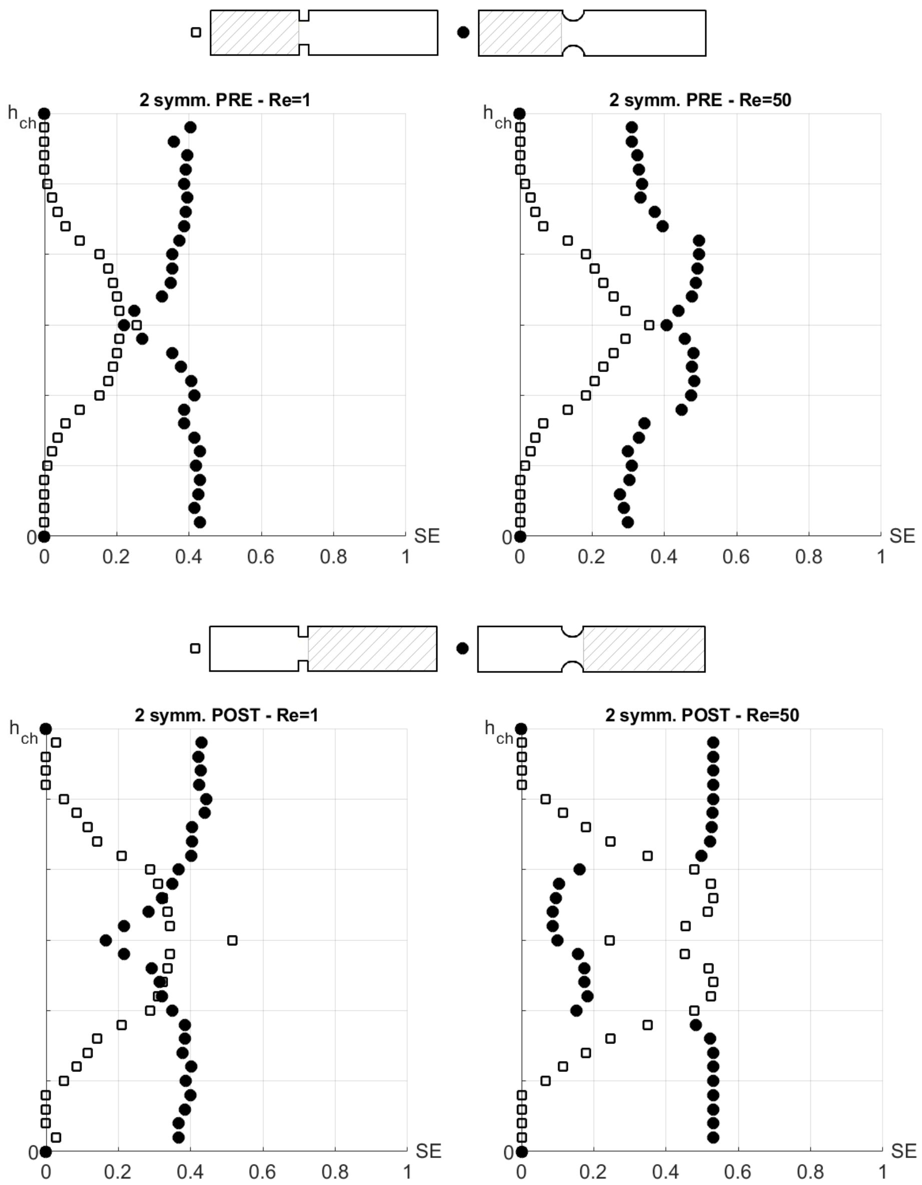

Fig. 4 SE computed on two cross-sections (proximal to the obstacle, upper panel; distal to the obstacle, lower panel) of two microchannels presenting obstacles with rectangular and semicircular shape, at *Re* = 1 and 50. Obstacles are symmetrically located with respect to the axis of the microchannels. h_{ch} is the general height of the channel.

In order to check for the robustness of SE with respect to the CFD grid cardinality (i.e. the number of nodes considered for the SE calculation), a sensitivity analysis was carried out where nodes were decimated. Technically, the average value of the SE was calculated considering the entire microchannel fluid domain as follows: (1) considering the 100% of the mesh grid elements; (2) considering only 50% of the mesh grid elements; (3) averaging the velocity values of two adjacent mesh grid elements. The percentage differences among the average SE values, summarized in Fig. 5 for microchannels with four different semicircular shape obstacle configurations, clearly show that a substantial reduction (50%) in the number of mesh grid elements weakly influences SE evaluation (with differences lower than 6%).

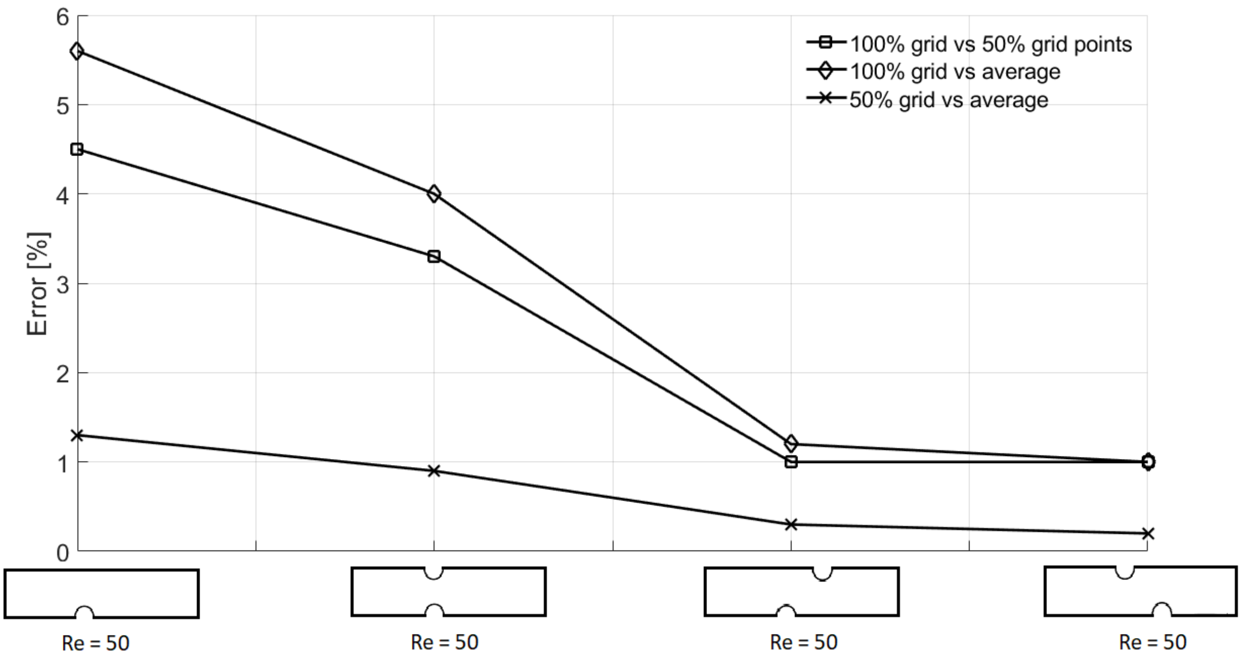

Fig. 5 Impact of the number of mesh grid elements on microchannel average SE values. The analysis was carried out considering the 100% and the 50% of the mesh grid elements, as well as averaging the

velocity values of two adjacent mesh grid elements. The results refer to four microchannels with different configurations of semicircular obstacles

4 Conclusions

In this study the fluid dynamics in microchannels with obstacles was investigated using the concept of entropy, here approached in a different way compared to the present state-of-the-art (Camesasca et al. 2006, Pozo et al. 2017, Rocha et al. 2008). The analysis suggests that a quantity linked to entropy, SE, is capable to discriminate among different shapes and configurations of obstacles within a microchannel. In the microfluidic field the capability to infer presence and configuration of obstacles in microsystems from SE differences between inflow and outflow sections could allow to monitor e.g. cells shape and growth in microbioreactors, as well as mixing of species in the microsystem itself. Applications other than biomicrofluidics, where fluid streamlines entropy can be employed to describe the physics within the microsystem just looking at SE input and output variations are manifold, ranging from microelectronics to chemistry (Ghaneifar et al. 2021, Shahsavar et al. 2020, Khalid et al. 2021). In this sense, the here presented results represent a starting point for future dedicated applications where the extraction of information on the processes occurring inside a not accessible system is critical.

Integrating statistical mechanics with information theory, in the long run will allow to establish a clearly distinguishable link between thermodynamics perturbation of a system and the level of interaction of the individual elements of which a system is made.

Conflicts of interest

The authors declare that they have no competing interests.

References

Ali HM (2020) Recent advancements in PV cooling and efficiency enhancement integrating phase change materials based systems – A comprehensive review. Sol Energy 197:163–198. https://doi.org/10.1016/j.solener.2019.11.075

Bilen K, Yapici S (2002) Heat transfer from a surface fitted with rectangular blocks at different orientation angle. Heat Mass Transfer 38:649–655. https://doi.org/10.1007/s002310100275

Camesasca M, Kaufman M, Manas-Zloczower I (2006) Quantifying fluid mixing with the Shannon entropy. Macromol Theory Simul 15:595–607. https://doi.org/10.1002/mats.200600037

Chen C-Y, Su J-H, Ali HM, Yan W-M, Amani M (2020) Effect of channel structure on the performance of a planar membrane humidifier for proton exchange membrane fuel cell. Int J Heat Mass Transfer 163:120522. https://doi.org/10.1016/j.ijheatmasstransfer.2020.120522

Cox SJ (2015) Simulations of bubble division in the flow of a foam past an obstacle in a narrow channel. Colloids Surf, A 473:104–108. https://doi.org/10.1016/j.colsurfa.2014.10.038

Eijkel JCT, van den Berg A (2005) Nanofluidics: what is it and what can we expect from it? Microfluid Nanofluid 1:249–267. https://doi.org/10.1007/s10404-004-0012-9

Ghaneifar M, Raisi A, Talebizadehsardari P (2021) Mixed convection heat transfer of Al_2O_3 nanofluid in a horizontal channel subjected with two heat sources. J Therm Anal Calorim 143:2761–2774. https://doi.org/10.1007/s10973-020-09887-2

Ikeda K, Matsumoto K (1989) Information theoretical characterization of turbulence. Phys Rev Lett 62:2265–2268. https://doi.org/10.1103/PhysRevLett.62.2265

Khalid SU, Babar H, Ali HM, Janjua MJ, Ali MA (2021) Heat pipes: progress in thermal performance enhancement for microelectronics. J Therm Anal Calorim 143:2227–2243. https://doi.org/10.1007/s10973-020-09820-7

Khasanov NA (2011) Acoustic oscillations of a gas near nested thin-walled cylindrical obstacles in a channel. J Appl Mech Tech Phys 52:577–584. https://doi.org/10.1134/S0021894411040109

Merdasi A, Ebrahimi S, Moosavi A, Shafii MB, Kowsary F (2018) Simulation of a falling droplet in a vertical channel with rectangular obstacles. Eur J Mech B Fluids 68:108–117. https://doi.org/10.1016/j.euromechflu.2017.11.002

Pennella F, Mastrangelo F, Gallo D, Massai D, Deriu MA, Falvo D'Urso Labate G, Bignardi C, Montevecchi F, Morbiducci U (2010) A survey of microchannel geometries for mixing of species in biomicrofluidics. In: Dias R, Lima R, Martins AA, Mata TM (eds.) Single and two-phase flows on chemical and biomedical engineering, 1st edn. Bentham Science Publishers, Sharjah, pp 548–578. https://doi.org/10.2174/978160805295011201010548

Pennella F, Rossi M, Ripandelli S, Rasponi M, Mastrangelo F, Deriu MA, Ridolfi L, Kähler CJ, Morbiducci U (2012) Numerical and experimental characterization of a novel modular passive micromixer. Biomed Microdevices 14:849–862. https://doi.org/10.1007/s10544-012-9665-4

Pozo JM, Geers AJ, Villa-Uriol M-C, Frangi AF (2017) Flow complexity in open systems: interlacing complexity index based on mutual information. J Fluid Mech 825:704–742. https://doi.org/10.1017/jfm.2017.392

Rocha LB, Adam RL, Leite NJ, Metze K, Rossi MA (2008) Shannon's entropy and fractal dimension provide an objective account of bone tissue organization during calvarial bone regeneration. Microsc Res Tech 71:619–625. https://doi.org/10.1002/jemt.20598

Sajjad U, Sadeghianjahromi A, Ali HM, Wang C-C (2020) Enhanced pool boiling of dielectric and highly wetting liquids - a review on enhancement mechanisms. Int Commun Heat Mass Transfer 119:104950. https://doi.org/10.1016/j.icheatmasstransfer.2020.104950

Shahsavar A, Ali HM, Mahani RB, Talebizadehsardari P (2020) Numerical study of melting and solidification in a wavy double-pipe latent heat thermal energy storage system. J Therm Anal Calorim 141:1785–1799. https://doi.org/10.1007/s10973-020-09864-9

Shannon CE (1948) A mathematical theory of communication. Bell Syst Tech J 27:379–423. https://doi.org/10.1002/j.1538-7305.1948.tb01338.x

Sözen A, Filiz Ç, Aytaç İ, Martin K, Ali HM, Boran K, Yetişken Y (2021) Upgrading of the performance of an air-to-air heat exchanger using graphene/water nanofluid. Int J Thermophys 42:35. https://doi.org/10.1007/s10765-020-02790-w

Tariq HA, Anwar M, Malik A, Ali HM (2020) Hydro-thermal performance of normal-channel facile heat sink using TiO_2-H_2O mixture (Rutile-Anatase) nanofluids for microprocessor cooling. J Therm Anal Calorim. https://doi.org/10.1007/s10973-020-09838-x

Wang X, Li C, Zhang Y, Ding W, Yang M, Gao T, Cao H, Xu X, Wang D, Said Z, Debnath S, Jamil M, Ali HM (2020) Vegetable oil-based nanofluid minimum quantity lubrication turning: Academic review and perspectives. J Manuf Processes 59:76–97. https://doi.org/10.1016/j.jmapro.2020.09.044

Yojina J, Ngamsaad W, Nuttavut N, Triampo D, Lenbury Y, Kanthang P, Sriyab S, Triampo W (2010) Investigating flow patterns in a channel with complex obstacles using the lattice Boltzmann method. J Mech Sci Technol 24:2025–2034. https://doi.org/10.1007/s12206-010-0712-x